Introduction to mechanical metamaterials and their effective properties

Xueyan Chen[1,2], Nicolas Laforge[1], Qingxiang Ji[1,2*], Huifeng Tan[2], Jun Liang[2,3], Gwenn Ulliac[1], Johnny Moughames[1], Samia Adrar[1], Vincent Laude[1], Muamer Kadic[1]

[1] *Institut FEMTO-ST, UMR 6174, CNRS, Université de Bourgogne Franche-Comté, 25000 Besançon, France*

[2] *National Key Laboratory of Science and Technology on Advanced Composites in Special Environments, Harbin Institute of Technology; 92 Xidazhi Street, Harbin, 150001, PR China*

[3] *Institute of Advanced Structure Technology, Beijing Institute of Technology, No.5 South Zhongguancun Street, Haidian District, Beijing, 100081, PR China*

Abstract

Metamaterials are rationally designed composites made of building blocks which are composed of one or more constituent materials. Metamaterial properties can go beyond those of the ingredient materials, both qualitatively and quantitatively. In addition, their properties can be mapped on some generalized continuum model. We present the general procedure of designing elastic metamaterials based on masses and springs. We show that using this simple approach we can design any set of effective properties including linear elastic metamaterials, – defined by bulk modulus, shear modulus, mass density – and non linear metamaterials, – with instabilities or programmable parts. We present designs and corresponding numerical calculations to illustrate their constitutive behavior. Finally, we discuss the addition of a thermal stimulus to mechanical metamate-

[1] jiqingxiang@hit.edu.cn

rials.

Keywords: Metamaterials, Effective parameters, Elasticity, Anisotropy, Waves, Cauchy elasticity, Navier equation.

2010 MSC: 00-01, 99-00

---

1. Introduction

For the last 50 years, a huge deal of effort has been made to design novel materials by chemical synthesis (graphene [1, 2, 3], carbon nanotubes [4, 5]), by structuration (composites, fibrous materials, multilayers)[6, 7, 8], or by topology optimization in quasi-static conditions [9] or for dynamical Bloch waves (phononic crystals)[10]. The ultimate goal has been to reach an improvement in stiffness or toughness, increase or decrease in the mass density, or to absorb/reflect or transmit energy [9, 11, 12]. Indeed, in aeronautics and the automotive industry for instance, it was necessary to decrease the weight of all parts leading to a fundamental change from metals to only aluminum, alloys and composites. It is, for example, almost impossible to find a car bumper made of metal today thanks to composites (mainly fibrous). The quest for a dynamical design response (sound and vibration absorption), firstly questioned by Brillouin, was deeply expanded after pioneering works by Yablonovitch [13, 14], Monkhorst[15], and Bloch[16]. Later, the introduction of functionalities designed by transformational elastodynamics and the wish of mapping more complex media onto generalized continua motivated the expansion from Cauchy elasticity to micropolar, micromorphic or Cosserat models (an effort started in the sixties by Eringen, Maugin and other precursors [17, 18]) led to the higher order gradient

theories of elasticity [19] and to the modification of the Newton's second law by Willis and Milton [20].

In this paper, we revisit these innovations from the perspective of metamaterial designs taken from the literature. First, we summarize for newcomers the different models used in elasticity. Second, we focus on linear elasticity and show that using masses and spring all mechanical properties can be independently designed. Third, we present an extension of linear metamaterials toward their use for non-linear wave absorption.

2. Elasticity equations

In this section we review the complexity of the description of mechanical materials and of their constitutive laws [21].

2.1. Hooke's spring law

In the seventeenth century, Robert Hooke formulated the first constitutive law in mechanics that states that the force, F, needed to extend or compress a spring by a distance d is given by $F = k\ d$, where k is a constant (the stiffness). This law can obviously be generalized to a vectorial force $\mathbf{F}$ connecting a general vector elongation in 3D space $\mathbf{d} = (d_1, d_2, d_3)$ by a matrix of spring constants $\mathbf{k}$ as $\mathbf{F} = \mathbf{k}\ \mathbf{d}$. It is well known that in the general case, the spring constant is a constant scalar (or a constant matrix), but that its magnitude can change depending on the load in a non linear way (either monotonically or not; see the section on non linear mechanics). In Figure 1 we illustrate the principles of linear and non-linear springs and continua, a concept that we will more clearly

describe later on. The scalar Hooke's law primarily relates linearly the tension of an homogeneous spring to its elongation (Fig. 1(a)). If the spring is made inhomogeneous along its length, such as in Fig. 1(b), then the relationship becomes non linear. Similarly, the homogeneous cube of Fig. 1(c) can often be modelled with the linear Hooke's law, but a structural spring such as depicted in Fig. 1(d) must be described using a non linear stiffness under large deformations. In the figure, the color scale represents the local vertical displacement with respect to the static equilibrium position under zero tension. The elongation d is the difference of the top displacement and the bottom displacement. Whereas in the first three cases the displacement field is basically a simple vertical gradient, in the structural spring case the displacement field varies in a more complex fashion.

Clearly, Hooke's approach can be justified only for simple spring-like geometries and for long bars. When all dimensions (pushing and lateral) of a material are comparable then this approach does not reflect properly the deformation of the body. Thus, a more general theory is required. It is called Cauchy elasticity from the contribution of Louis Cauchy to the definition of the stress tensor replacing the simple applied force by a quantity homogeneous to a force per surface area (thus with the units of pressure). Figure 2 illustrates the different components of the Cauchy stress tensor exerted on an infinitesimal cubic volume.

The stress tensor defined graphically in Fig. 2 obeys the fundamental law of conservation of linear momentum. Combined with the conservation of angular

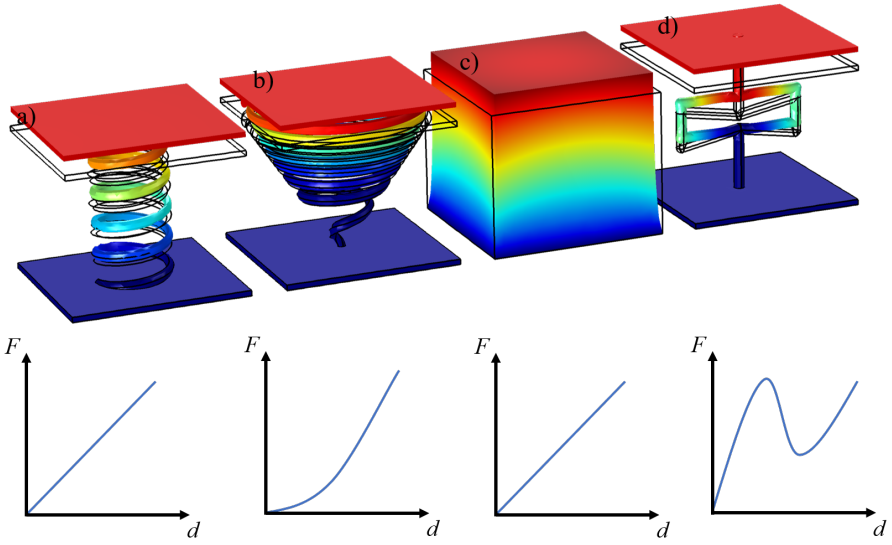

Figure 1: Under uniaxial tension, the deformations of (a) a linear spring, (b) a non linear spring, (c) an homogeneous cube, and (d) a geometrically non linear spring are depicted, respectively. The color scale measures the vertical displacement, from blue (no displacement) to red (maximum displacement). For the finite element computations, the bottom surface is clamped and a force F directed upward is applied at the top surface. The thin lines are for the structures at rest. Under each panel, a schematic force-elongation curve is displayed.

momentum, the stress tensor takes a symmetric form with only six independent parameters, rather than nine, and may thus be written:

$$\begin{bmatrix} \sigma_{11} & \sigma_{12} & \sigma_{13} \\ \sigma_{21} & \sigma_{22} & \sigma_{23} \\ \sigma_{31} & \sigma_{32} & \sigma_{33} \end{bmatrix} = \begin{bmatrix} \sigma_1 & \sigma_6 & \sigma_5 \\ \sigma_6 & \sigma_2 & \sigma_4 \\ \sigma_5 & \sigma_4 & \sigma_3 \end{bmatrix} \tag{1}$$

where the diagonal entries σ_1, σ_2 and σ_3 are the normal stresses, and the off-diagonal entries $\sigma_{12} = \sigma_6$, $\sigma_{13} = \sigma_5$ and $\sigma_{23} = \sigma_4$ are the orthogonal shear stresses.

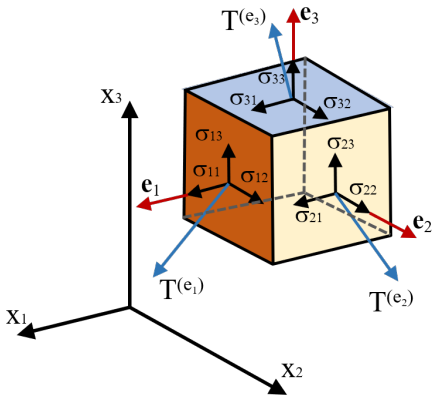

Figure 2: Illustration of the elements of the Cauchy tensor and of the orientation convention. In a Cartesian coordinate system, the stress vectors applying on each elemental plane, $T^{(e_1)}$, $T^{(e_2)}$, and $T^{(e_3)}$ can be can be decomposed into a normal component and two shear components measured along the three principal axes.

Next, the infinitesimal strain tensor for a displacement field $\mathbf{u}$ is defined by:

$$\boldsymbol{\varepsilon} = \frac{1}{2}[\nabla \mathbf{u} + (\nabla \mathbf{u})^T].$$

By construction this tensor is also symmetric. In component form, it writes as

$$\varepsilon_{ij} = \frac{1}{2}\left(u_{i,j} + u_{j,i}\right), \qquad i,j = 1,2,3,$$

and the notation $u_{i,j} = \frac{\partial u_i}{\partial x_j}$. Therefore, the displacement gradient can alternatively be expressed as

$$\nabla \mathbf{u} = \boldsymbol{\varepsilon} + \boldsymbol{\gamma}$$

with a skew symmetric tensor $\boldsymbol{\gamma}$ also called the rotation tensor:

$$\boldsymbol{\gamma} = \frac{1}{2}[\nabla \mathbf{u} - (\nabla \mathbf{u})^T].$$

Finally the constitutive equation between stress and stain tensors is given by

the generalized Hooke's law as

$$\boldsymbol{\sigma} = \mathsf{C} : \boldsymbol{\varepsilon},$$

with $\boldsymbol{\sigma}$ Cauchy's stress tensor, $\boldsymbol{\varepsilon}$ the infinitesimal strain tensor, and C a fourth-order elasticity tensor. The latter must obey certain properties of tensors such as symmetries and positive definiteness.

Sometimes it is difficult to model lattice metamaterials with continuum mechanics, especially if bars get very thin and numerous. For this prupose, it is important to note that simplified theories exist, e.g. Timoshenko's and Euler-Bernouilli beam theories. However, in the quest of an efficient implementation they are not practical compared to finite element models. Anyway, an extensive and specific literature exists and has been used for the design of metamaterials [22, 23, 24, 25, 26].

2.2. Navier's equation

Once a rigid or deformable body is in motion, Newton's second law can be written as follows (omitting possible external forces):

$$\nabla \cdot \boldsymbol{\sigma} = \rho \, \frac{\partial^2 \mathbf{u}}{\partial t^2} \tag{2}$$

with ρ the mass density and t the time variable. If the elastic body is isotropic, then

$$\mathsf{C}_{ijkl} = \lambda \delta_{ij} \delta_{kl} + 2\mu \delta_{ij}, \tag{3}$$

where Lamé's parameters λ and μ can be expressed in terms of Poisson's ratio ν and Young's modulus E as

$$\lambda = \frac{E\nu}{(1+\nu)(1-2\nu)}, \mu = \frac{E(1-\nu)}{(1+\nu)(1-2\nu)}. \tag{4}$$

In the time-harmonic regime Navier's equation at angular frequency ω is

$$\nabla \cdot \boldsymbol{\sigma} = -\rho\,\omega^2\,\mathbf{u}. \tag{5}$$

3. Linear Mechanical metamaterials

3.1. Isotropic metamaterials

In the isotropic case, the effective elasticity tensor that describes the elastic properties of a solid metamaterial is very simple and in fact can be decomposed a form with only two eigenvalues (see Milton [27] and Banerjee [28]). Here, we describe how to design the most simple isotropic mechanical metamaterial (as a remark, isotropy in mechanics is not as simple as in crystallography, since space groups must be considered instead of point groups in order to describe symmetry). We start from the ideal pentamode metamaterials introduced by Milton and Cherkaev [27], as shown in Fig. 3. Pentamodes are expected to avoid the coupling of compression and shear waves due to their extremely large bulk modulus, B, in comparison with the shear modulus, G [27, 29]. However, it is almost impossible to fabricate such ideal pentamodes due to infinitely small connections between cones. In 2012, Kadic et al. realized pentamodes experimentally by modifying the diameter of thin and thick ends of double cones [29]. They investigated the effect of the overlap volume on the ratio B/G. They

found that increasing the overlap volume stabilizes the structures, yet at the same time decreasing the ratio.

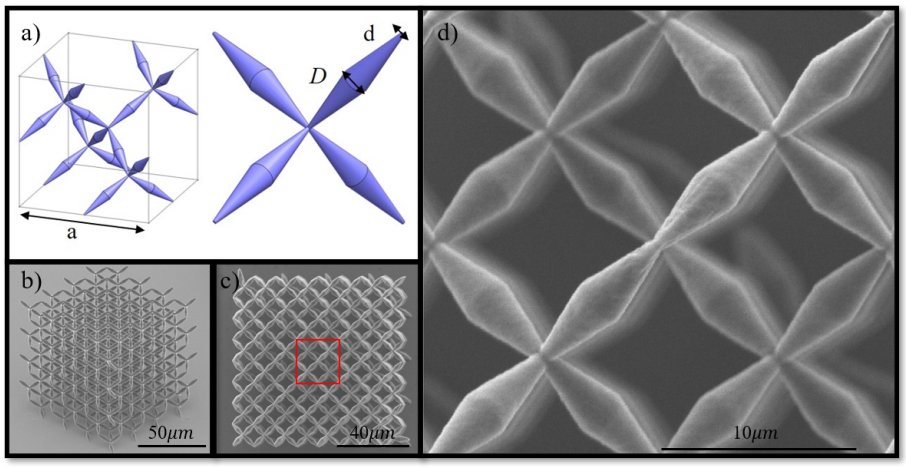

Figure 3: a) An ideal periodic unit cell of a pentamode metamaterial with constant length a and a modified pentamode with a smaller diameter, d, at connecting parts of the double-cone strut, and a bigger diameter, D, of the middle part. 3D view (b) and magnified front view (c) electron micrograph of a pentamode truss micro-lattice metamaterial fabricated by dip-in three-dimensional direct-laser-writing (DLW) optical lithography. Front view electron micrograph (d) of an unit cell of the metamaterial part which is highlighted with a red square in (c). The samples chosen reproduce those discussed originally in Ref. [29].

Figs. 3 (b) and (c) show 3D view and magnified front view electron micrographs of an optimal pentamode truss micro-lattice metamaterial fabricated by dip-in three-dimensional direct-laser-writing (DLW) optical lithography. These structures are experimentally validated to possess an extremely large B/G ratio which can be also observed in Fig. 5 a). Fig. 4 and Fig. 5 b) illustrate how to independently control the bulk modulus B by connecting the middle part of double cones with soft loose springs. One can also fulfill the goal to control

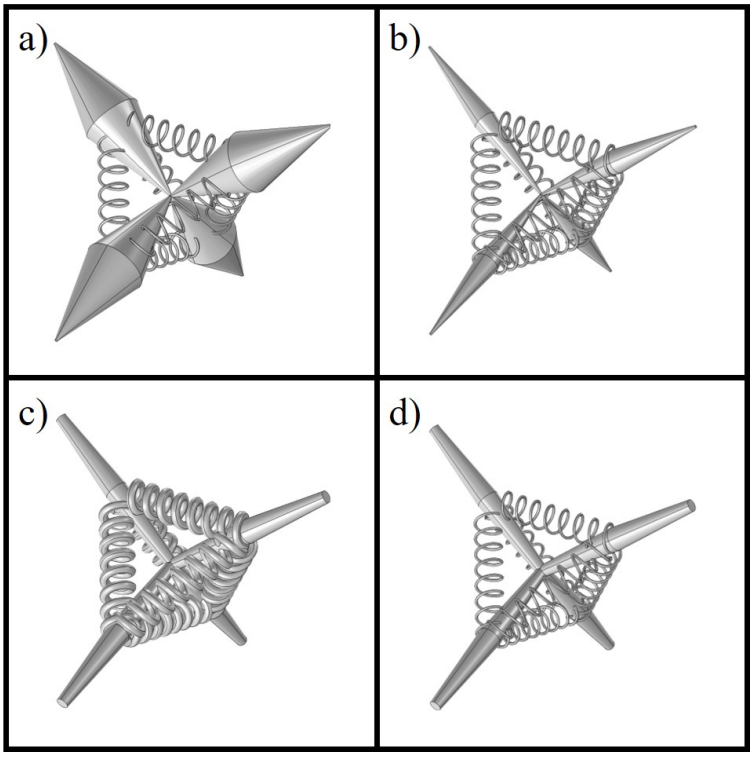

Figure 4: Illustration of optimal pentamodes with (a) a larger diameter D and additional loose springs, (b) additional loose springs, (c) a larger diameter d and additional dense springs and d) a larger diameter d and additional loose springs.

density by using parallel springs while enlarging the diameter d. By replacing loose springs with dense springs, it is easy to keep the bulk modulus B and to enhance the capacity to resist shear loading.

Actually, we can make pentamode metamaterials isotropic by adapting the optimal method presented by Buckmann *et al.* [31]. We can relate the elastic modulus, the shear modulus and Poisson's ratio to three phase velocities v of the pentamode material, which are chosen either purely longitudinally or transversely polarized, in the FM direction or [110] direction. We thus get a suf-

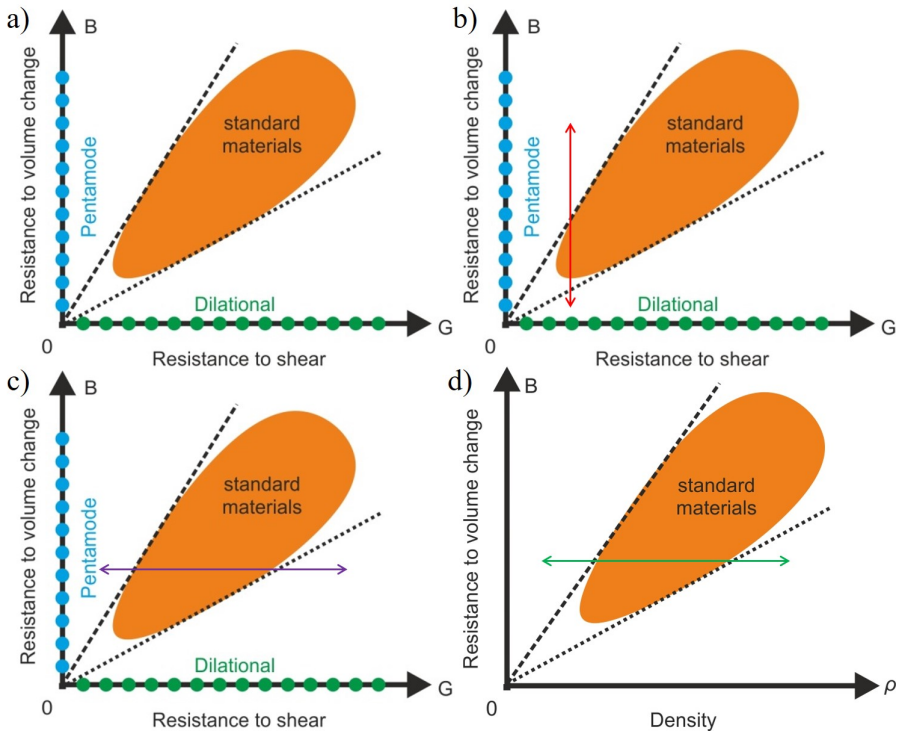

Figure 5: Milton's maps of (a) pentamode metamaterials and (b), (c) optimal pentamode metamaterials with different geometrical parameters. Ashby's map (d) of optimal pentamode metamaterials. This figure is inspired by Ref. [30].

ficient condition for isotropy as $v^L_{110} = v^{T,xy}_{110}$. This condition can be undertood as follows: the phase velocity of the longitudinal wave along the crystallographic direction [110] equals the phase velocity of the transverse wave along the same direction. The condition can be achieved by adjusting geometrical parameters or by adding additional springs. All in all, we obtain a possible way to control the 3 independent mechanical parameters and to make pentamodes isotropic by adjusting different parts of the periodic unit cell.

4. Nonlinear mechanical metamaterials

In the regime of large deformations, the stress-strain response of mechanical metamaterials [32, 33, 34] always goes through a sequence of increases [35, 36] or decreases [37, 38], and steady [39, 40, 41] or damping [42, 43] variations. Globally, the part of the graph extending beyond the initial elastic region describes the mechanical nonlinearity. Scientists usually pay much attention to the elastic region for load-bearing mechanical metamaterials [38, 43], whereas nonlinearity is important for energy absorption mechanical metamaterials [39, 43] and programmable metamaterials [44, 11]. Nonlinearity arises from two aspects, either geometrical (structural) nonlinearity or the nonlinearity of the parent materials used for building the metamaterial [45]. Geometrical nonlinearity, which is mainly determined by the topological structure and geometrical parameters, exists in systems that sustain large deformations. Geometrical structures, such as truss lattices [35, 40], shell lattices [42, 43] and plate lattices [46, 47] have to abide by two different deformation criteria: stretching dominated or bending dominated [48]. Different geometrical parameters will yield different failure modes, including stiffening or softening plastic yield [38], plastic collapse [35], linear and nonlinear buckling [39, 43], and so on. In a similar way, the mechanical properties, especially in the nonlinear region, of the parent materials also affect the failure modes of mechanical metamaterials. Material nonlinearity works only after the deformation of the parent materials has gone beyond the elastic region. Plastic yield will dominate the failure of most metals and polymers. However, brittle failure will be most common for ceramics, composite

materials, and other ceramic-like materials. Material properties and the topological structure together with geometrical parameters decide the failure models, that is the nonlinear response, of mechanical metamaterials.

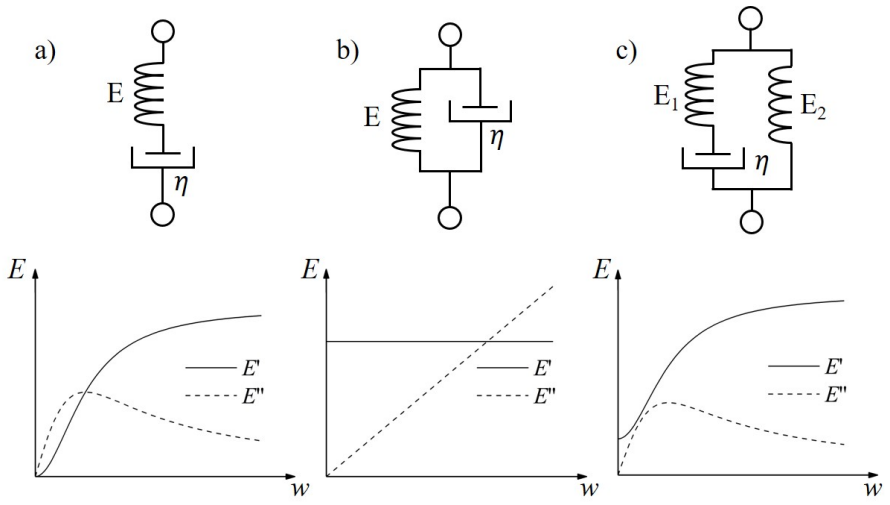

Figure 6: a) Maxwell, b) Voigt and c) the standard linear solid simplified elastic-viscous models are depicted in analogy with equivalent electrical circuits. Young's modulus E is analogous to a real-valued admittance, whereas viscosity contributes a $i\omega\eta$ admittance similar to a capacitance. The resulting relationship between dynamic modulus and angular frequency is depicted below each equivalent circuit model (see text for their expressions).

Viscous materials, for which the relationship between stress and strain depends on time, provide another possibility to design energy absorption, energy dissipation, and vibration suppression metamaterials. Their energy dissipation capacity highly depends on the angular frequency. Several mathematical models have been proposed to describe such dispersive relationships. The Maxwell loss model [49, 50] is probably the oldest viscoelastic model and can be represented by a purely viscous damper and a purely elastic spring connected in series, as

shown in Fig. 6 (a). The dynamic modulus $E^*(\omega) = E' + iE''$ is obtained following the rules for admittance in equivalent circuits. In the case of the Maxwell model,

$$\frac{1}{E^*} = \frac{1}{E} + \frac{1}{i\omega\eta} \tag{6}$$

which yields

$$E' = \frac{\tau^2\omega^2}{\tau^2\omega^2 + 1}E, \quad E'' = \frac{\tau\omega}{\tau^2\omega^2 + 1}E, \tag{7}$$

with $\tau = \eta/E$. If we connect elastic and viscous elements in parallel, as in Fig. 6 (b), we get the generalized Kelvin-Voigt model [49, 50]

$$E^* = E + i\omega\eta. \tag{8}$$

Then obviously $E' = E$ and $E'' = \omega\eta$. Combining a serial Maxwell branch in parallel with a purely elastic branch, the more realistic model of the standard linear solid is obtained, as depicted in Fig. 6 (c). The model contains two independent elastic elements, E_1 and E_2, and a viscous element η, and is also known as the Zener model[49, 50, 51]. The complex dynamic modulus is

$$E^*(\omega) = \left(\frac{1}{E_1} + \frac{1}{i\omega\eta}\right)^{-1} + E_2, \tag{9}$$

leading to

$$E'(\omega) = \frac{\tau^2\omega^2}{\tau^2\omega^2 + 1}E_1 + E_2, \tag{10}$$

$$E''(\omega) = \frac{\tau\omega}{\tau^2\omega^2 + 1}E_1. \tag{11}$$

Fig. 6 depicts the three previous elastic-viscous models and the corresponding relationships between dynamics modulus and vibration frequency. The equations are simple enough but often prove insufficient. For instance, the Maxwell

model successfully captures the evolution of the imaginary dynamic modulus as a function of vibration frequency, but fails to describe the dependence of the real part on frequency. It should be noted that any solid material must have a non zero elastic modulus in the absence of vibrations, i.e. at the zero frequency. Hence, the Maxwell loss model is not physical in the limit of low frequencies. Finally, the Kelvin-Voigt model is too ideal to describe nonlinear variations of the dynamic modulus.

4.1. Tailoring the stress-strain curve

A central issue of mechanical metamaterial design is indeed to tailor the stress-strain curve to follow given shapes chosen in order to meet given requirements [35, 39, 46]. As outlined in the previous section, the geometrical structure is one of most important factors in metamaterial design. Here, we will give three examples to illustrate how to tailor the stress-strain curve by optimizing the structure.

Let us start from a conventional spring which is the most basic elastic element in a mechanical metamaterial. When a conventional spring is compressed or stretched from its rest position (strained), a stress distribution appears along the length. Fig. 1(a) illustrates the force versus elongation curve. The spring constant is almost a constant as long as deformation does not go beyond spring stoke. Under certain circumstances, however, a spring constant increasing with applied strain is needed. In this case, replacing the constant spacing spring coils with graded spacing spring coils, or replacing the constant major radius with an increasing major radius, a progressive rate spring can be obtained, as Fig.

1(b) depicts.

Second, the simple cubic solid structure, that is a base element in 3D mechanical metamaterials, can be used to implement any geometrical structure by periodic repetition of a unit cell. Fig. 1(c) shows the deformation and the corresponding stress-strain curve of an homogeneous cubic unit cell under tension. Clearly, Poisson's ratio is positive and a conventional elastic-plastic tensile response is obtained. However, the structure [32] shown in Fig. 1(d), which is composed of several relatively small simple cubic elements, has a totally different deformation behavior: it is auxetic (Poisson's ratio is negative). Moreover, the failure mode changes from elastic-plastic to plastic bending. Note that such mechanical behavior is unusual in natural materials.

Third, we consider the control of the failure mode of mechanical metamaterials. The body centered cubic (BCC) shell-lattice metamaterial depicted in Fig. 7 has high stiffness, high strength, and large specific energy absorption at low relative density [52]. The compressive failure mode of the metamaterial, either dominated by plastic yield or buckling, is affected by the geometrical parameters defining the structure, including the spherical node radius R, the cylindrical strut radius r, the smooth connecting shell radius r_0, the cylindrical strut length l_0, the total length l, and thickness t_1. These geometrical parameters are not independent: we have $r_0 = 2R - r$ and $l = l_0 + 2\sqrt{3}(R - r)$. Further fixing the total length of the shell strut and setting the relative density to 0.05, only two independent parameters are left, for instance the spherical node radius R and the smooth connecting shell radius r_0. After topology optimization,

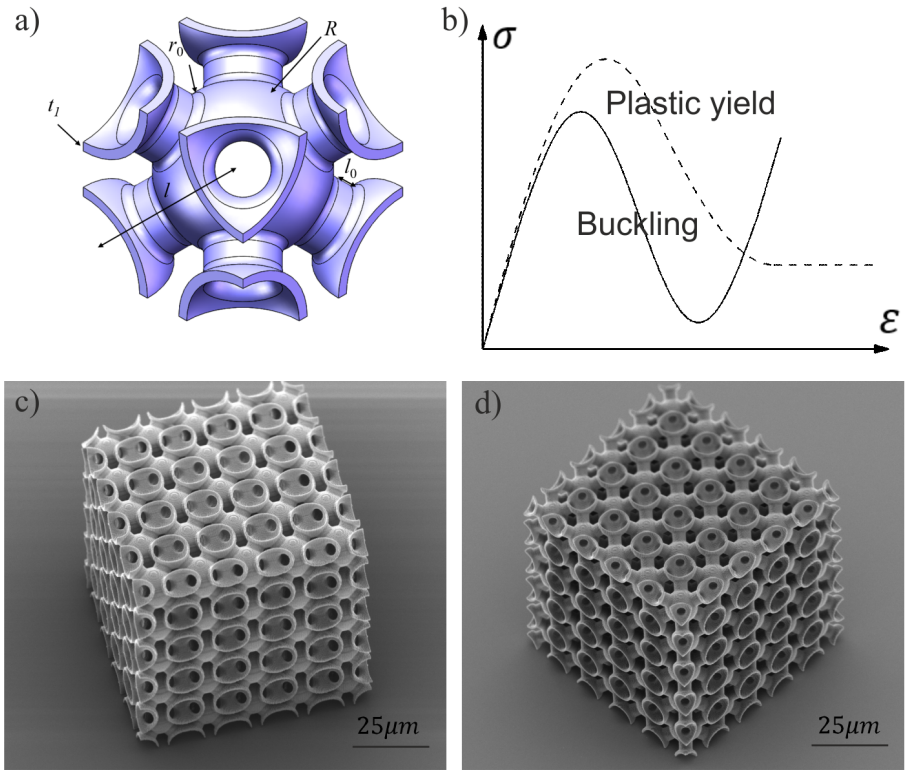

Figure 7: Body centered cubic (BCC) shell-lattice metamaterial. a) A unit cell is depicted along with its geometrical parameters. b) Two different failure models can be observed for the shell-lattice material, either plastic yield or buckling. The optimal designs obtained for c) energy absorption and d) bearing load were fabricated by two-photon lithography.

we obtained two different functional shell metamaterials: a buckling dominated metamaterial ($R/r = 2.3$ and $l_0/(l - l_0) = 0.1$) and a yield dominated metamaterial ($R/r = 2.5$ and $l_0/(l - l_0) = 0.2$). The buckling dominated metamaterial can almost recover 92% of its original shape after compressions in excess of 60% strain, which makes it a good candidate for energy absorption. The yield dominated metamaterial has higher stiffness, higher strength and better load bearing

capacity. These examples encourage one to make possible the impossible.

4.2. Material non linearities and their use for energy absorption

Nonlinear metamaterials are widely used in our daily life for energy absorption [53, 54, 55, 56]. Aiming at absorbing as much energy as possible, nonlinear metamaterials were usually designed to obtain a relatively large peak force with large deformation [35, 55, 57]. Most metamaterials utilize plastic deformation or brittle fracture of micro-struts [37], shell [43] or plate [46, 47] to dissipate a large amount of energy. Stretching dominated metamaterials [43, 46, 47], which are maybe the most famous plastic yield metamaterials, have been proven to possess extraordinary loading bear capacity and energy absorption at high relative density. In contrast, bending dominated metamaterials [35, 41], which make use of plastic bending joint, allow for large deformation and provide relatively large and nearly constant stress area in the nonlinear region at low relative density. In addition, reusable energy metamaterials [58, 39, 59] were proposed to extend their life span. By utilizing elastic buckling of shell, straight strut and curved beam, reusable energy metamaterials were shown to present unusual features including mechanical multi-stability [60, 61], close to 100 percent recovery after unloading [39, 58, 55], and controllable mechanical response [44].

5. Thermomechanical metamaterials

Systems placed in a thermal environment are sensitive to temperature changes of their surroundings. An ambient temperature change ΔT will cause a thermal

strain $\alpha_{ij}\Delta T$ in an elastic solid due to thermal expansion. Generally, thermal expansion is described by a symmetric tensor of rank two

$$\alpha_{ij} = \begin{bmatrix} \alpha_{11} & \alpha_{12} & \alpha_{13} \\ \alpha_{12} & \alpha_{22} & \alpha_{23} \\ \alpha_{13} & \alpha_{23} & \alpha_{33} \end{bmatrix}. \tag{12}$$

For isotropic solids, the thermal expansion tensor is proportional to the identity matrix, $\alpha_{ij} = \alpha \boldsymbol{I}$, where $\boldsymbol{I}$ is the rank-two identity matrix and α is the thermal length expansion defined by

$$\alpha = \frac{1}{L}\frac{\partial L}{\partial T}. \tag{13}$$

In the elastic stress-strain relation, thermal strain has to be subtracted from total strain, leading to the relation

$$\sigma_{ij} = C_{ijkl}\left(\varepsilon_{kl} - \alpha_{kl}\Delta T\right) \tag{14}$$

or, in the case of isotropic solids,

$$\sigma_{ij} = 2\mu\varepsilon_{ij} + \lambda\varepsilon_{ij}\delta_{ij} - (2\mu + 3\lambda)\,\alpha\Delta T\delta_{ij}. \tag{15}$$

Note that the temperature dependence of the elastic constants was neglected in the above equations.

220 Temperature variations can result both in thermal expansion and in geometry changes, which can be problematic in temperature-sensitive applications that require thermal stability like space frame trusses, satellite antennas and space crafts [62, 63]. Alternatively, thermal expansion can also be tailored to achieve some required thermal deformation and behavior. Material systems

and structures can be deliberately designed to deform in a controllable manner in response to a temperature stimulus. Applications based on this principle include morphing structures [64], large reversible shape changing components [65], micro-actuators [66], self-assembly systems [67], grippers for soft micro-robotics [68], biology devices [69], and so on.

Generally, those applications bring in demands on controllable coefficients of thermal expansion (CTE), e.g. large, positive, negative or zero thermal expansion materials and structures. Many efforts have been made to create architectured materials with tunable CTE using two constituents with widely different thermal expansion combined in space. Different concepts were proposed under this approach and each has its working principle and specific advantages. One major concept is utilizing the bending-dominated bi-material strip, based on which some researchers proposed cellular solid structures with unbounded thermal expansion [70, 71]. Other concepts include stretch-dominated structures composed of nested double-parallel units with large stiffness [71], flexure blade structures with high CTE tunability [72], and tetrahedron structure combined with sizable CTE tunability and large stiffness [73, 74]. Another major approach is to generate CTE tunability via topology optimization [75, 76, 77]. Structures obtained following this method are generally more complicated. Finally, using 3D printing technologies, researchers have managed to directly print metamaterials with controllable thermal expansion and have achieved rather high but negative thermal expansion coefficients [72, 78, 79].

6. Conclusion

In this paper, we have presented general procedures to design mechanical metamaterials in both the linear and the non linear regimes using an effective medium approach based on simple mechanical models. We have emphasized the complexity and the opportunities in the nonlinear case if one uses viscosity or plasticity. Finally, we have summarized proposals aiming at using an external stimulus (variation of temperature) to change the shape of designed metamaterials.

Acknowledgments

We thank Graeme W. Milton (Utah Univ., USA) and Martin Wegener (KIT, Germany) for stimulating discussions. We acknowledge Marina Raschetti, Roland Salut, and Jean-Marc Cote for technical help. This work was partly supported by the french RENATECH network and its FEMTO-ST technological facility. We acknowledge support by the EIPHI Graduate School (contract "ANR-17-EURE-0002") and the French Investissements d'Avenir program, project ISITE-BFC (contract ANR-15-IDEX-03). This work was partly supported by the french RENATECH network and its FEMTO-ST technological facility. This work was supported in part by the Foundation for Innovative Research Groups of the National Natural Science Foundation of China (grant numbers 11421091 and 11732002) and by the Fundamental Research Funds for the Central Universities (grant number HIT.MKSTISP.2016 09).

References

[1] M. J. Allen, V. C. Tung, R. B. Kaner, Honeycomb carbon: a review of graphene, Chemical reviews 110 (1) (2009) 132–145.

[2] Y. Shao, J. Wang, H. Wu, J. Liu, I. A. Aksay, Y. Lin, Graphene based electrochemical sensors and biosensors: a review, Electroanalysis: An International Journal Devoted to Fundamental and Practical Aspects of Electroanalysis 22 (10) (2010) 1027–1036.

[3] M. Yi, Z. Shen, A review on mechanical exfoliation for the scalable production of graphene, Journal of Materials Chemistry A 3 (22) (2015) 11700–11715.

[4] G. Mittal, V. Dhand, K. Y. Rhee, S.-J. Park, W. R. Lee, A review on carbon nanotubes and graphene as fillers in reinforced polymer nanocomposites, Journal of Industrial and Engineering Chemistry 21 (2015) 11–25.

[5] A. D. Moghadam, E. Omrani, P. L. Menezes, P. K. Rohatgi, Mechanical and tribological properties of self-lubricating metal matrix nanocomposites reinforced by carbon nanotubes (cnts) and graphene–a review, Composites Part B: Engineering 77 (2015) 402–420.

[6] J. J. Carruthers, A. Kettle, A. Robinson, Energy absorption capability and crashworthiness of composite material structures: a review, Applied Mechanics Reviews 51 (10) (1998) 635–649.

[7] D. Liu, Y. Tang, W. Cong, A review of mechanical drilling for composite laminates, Composite structures 94 (4) (2012) 1265–1279.

[8] R. F. Gibson, A review of recent research on mechanics of multifunctional composite materials and structures, Composite structures 92 (12) (2010) 2793–2810.

[9] X. Yu, J. Zhou, H. Liang, Z. Jiang, L. Wu, Mechanical metamaterials associated with stiffness, rigidity and compressibility: A brief review, Progress in Materials Science 94 (2018) 114–173.

[10] A. Srivastava, Elastic metamaterials and dynamic homogenization: a review, International Journal of Smart and Nano Materials 6 (1) (2015) 41–60.

[11] K. Bertoldi, V. Vitelli, J. Christensen, M. van Hecke, Flexible mechanical metamaterials, Nature Reviews Materials 2 (11) (2017) 17066.

[12] J.-H. Lee, J. P. Singer, E. L. Thomas, Micro-/nanostructured mechanical metamaterials, Advanced materials 24 (36) (2012) 4782–4810.

[13] E. Yablonovitch, Photonic band-gap structures, JOSA B 10 (2) (1993) 283–295.

[14] E. Yablonovitch, T. Gmitter, K.-M. Leung, Photonic band structure: The face-centered-cubic case employing nonspherical atoms, Physical review letters 67 (17) (1991) 2295.

[15] H. J. Monkhorst, J. D. Pack, Special points for brillouin-zone integrations, Physical review B 13 (12) (1976) 5188.

[16] P. E. Blöchl, O. Jepsen, O. K. Andersen, Improved tetrahedron method for brillouin-zone integrations, Physical Review B 49 (23) (1994) 16223.

[17] A. C. Eringen, E. S. Suhubi, S. Cowin, Elastodynamics (volume 1, finite motions), Journal of Applied Mechanics 42 (1975) 748.

[18] G. A. Maugin, Applications of an energy-momentum tensor in nonlinear elastodynamics: Pseudomomentum and eshelby stress in solitonic elastic systems, Journal of the Mechanics and Physics of Solids 40 (7) (1992) 1543–1558.

[19] J. Achenbach, Wave propagation in elastic solids, Vol. 16, Elsevier, 2012.

[20] G. W. Milton, J. R. Willis, On modifications of newton's second law and linear continuum elastodynamics, Proceedings of the Royal Society A: Mathematical, Physical and Engineering Sciences 463 (2079) (2007) 855–880.

[21] M. Kadic, G. W. Milton, M. van Hecke, M. Wegener, 3d metamaterials, Nature Reviews Physics (2019) 1.

[22] P. Martinsson, A. Movchan, Vibrations of lattice structures and phononic band gaps, Quarterly Journal of Mechanics and Applied Mathematics 56 (1) (2003) 45–64.

[23] D. Colquitt, I. Jones, N. Movchan, A. Movchan, Dispersion and localization of elastic waves in materials with microstructure, Proceedings of the Royal

Society A: Mathematical, Physical and Engineering Sciences 467 (2134) (2011) 2874–2895.

[24] A. Piccolroaz, A. Movchan, Dispersion and localisation in structured rayleigh beams, International Journal of Solids and Structures 51 (25-26) (2014) 4452–4461.

[25] A. N. Norris, Low-frequency dispersion and attenuation in partially saturated rocks, The Journal of the Acoustical Society of America 94 (1) (1993) 359–370.

[26] C. Findeisen, J. Hohe, M. Kadic, P. Gumbsch, Characteristics of mechanical metamaterials based on buckling elements, Journal of the Mechanics and Physics of Solids 102 (2017) 151–164.

[27] G. W. Milton, A. V. Cherkaev, Which elasticity tensors are realizable?, Journal of engineering materials and technology 117 (4) (1995) 483–493.

[28] B. Banerjee, An introduction to metamaterials and waves in composites, Crc Press, 2011.

[29] M. Kadic, T. Bückmann, N. Stenger, M. Thiel, M. Wegener, On the practicability of pentamode mechanical metamaterials, Applied Physics Letters 100 (19) (2012) 191901.

[30] M. Kadic, T. Bückmann, R. Schittny, M. Wegener, Metamaterials beyond electromagnetism, Reports on Progress in Physics 76 (12) (2013) 126501.

[31] T. Bückmann, R. Schittny, M. Thiel, M. Kadic, G. W. Milton, M. Wegener, On three-dimensional dilational elastic metamaterials, New Journal of Physics 16 (3) (2014) 033032.

[32] T. Bückmann, N. Stenger, M. Kadic, J. Kaschke, A. Frölich, T. Kennerknecht, C. Eberl, M. Thiel, M. Wegener, Tailored 3d mechanical metamaterials made by dip-in direct-laser-writing optical lithography, Advanced Materials 24 (20) (2012) 2710–2714.

[33] T. Frenzel, M. Kadic, M. Wegener, Three-dimensional mechanical metamaterials with a twist, Science 358 (6366) (2017) 1072–1074.

[34] I. Fernandez-Corbaton, C. Rockstuhl, P. Ziemke, P. Gumbsch, A. Albiez, R. Schwaiger, T. Frenzel, M. Kadic, M. Wegener, New twists of 3d chiral metamaterials, Advanced Materials (2019) 1807742.

[35] R. Gümrük, R. Mines, Compressive behaviour of stainless steel micro-lattice structures, International Journal of Mechanical Sciences 68 (2013) 125–139.

[36] T. Tancogne-Dejean, D. Mohr, Elastically-isotropic truss lattice materials of reduced plastic anisotropy, International Journal of Solids and Structures 138 (2018) 24–39.

[37] T. Tancogne-Dejean, D. Mohr, Stiffness and specific energy absorption of additively-manufactured metallic bcc metamaterials composed of tapered beams, International Journal of Mechanical Sciences 141 (2018) 101–116.

[38] V. S. Deshpande, N. A. Fleck, M. F. Ashby, Effective properties of the octet-truss lattice material, Journal of the Mechanics and Physics of Solids 49 (8) (2001) 1747–1769.

[39] T. Frenzel, C. Findeisen, M. Kadic, P. Gumbsch, M. Wegener, Tailored buckling microlattices as reusable light-weight shock absorbers, Advanced Materials 28 (28) (2016) 5865–5870.

[40] T. Tancogne-Dejean, A. B. Spierings, D. Mohr, Additively-manufactured metallic micro-lattice materials for high specific energy absorption under static and dynamic loading, Acta Materialia 116 (2016) 14–28.

[41] X. Cao, S. Duan, J. Liang, W. Wen, D. Fang, Mechanical properties of an improved 3d-printed rhombic dodecahedron stainless steel lattice structure of variable cross section, International Journal of Mechanical Sciences 145 (2018) 53–63.

[42] S. C. Han, J. W. Lee, K. Kang, A new type of low density material: Shellular, Advanced Materials 27 (37) (2015) 5506–5511.

[43] C. Bonatti, D. Mohr, Smooth-shell metamaterials of cubic symmetry: Anisotropic elasticity, yield strength and specific energy absorption, Acta Materialia 164 (2019) 301–321.

[44] B. Florijn, C. Coulais, M. van Hecke, Programmable mechanical metamaterials, Physical review letters 113 (17) (2014) 175503.

[45] L. J. Gibson, M. F. Ashby, Cellular solids: structure and properties, Cambridge university press, 1999.

[46] T. Tancogne-Dejean, M. Diamantopoulou, M. B. Gorji, C. Bonatti, D. Mohr, 3d plate-lattices: An emerging class of low-density metamaterial exhibiting optimal isotropic stiffness, Advanced Materials 30 (45) (2018) 1803334.

[47] J. Berger, H. Wadley, R. McMeeking, Mechanical metamaterials at the theoretical limit of isotropic elastic stiffness, Nature 543 (7646) (2017) 533.

[48] V. Deshpande, M. Ashby, N. Fleck, Foam topology: bending versus stretching dominated architectures, Acta materialia 49 (6) (2001) 1035–1040.

[49] R. S. Lakes, Viscoelastic solids, Vol. 9, CRC press, 1998.

[50] R. Christensen, Theory of viscoelasticity: an introduction, Elsevier, 2012.

[51] C. M. Zener, S. Siegel, Elasticity and anelasticity of metals., The Journal of Physical Chemistry 53 (9) (1949) 1468–1468.

[52] X. Chen, Q. Ji, J. Wei, H. Tan, J. Yu, P. Zhang, V. Laude, M. Kadic, Light-weight shell-lattice metamaterials for mechanical shock absorption, International Journal of Mechanical Sciences 169 (2020) 105288.

[53] G. Lu, T. Yu, Energy absorption of structures and materials, Elsevier, 2003.

[54] L. Salari-Sharif, T. A. Schaedler, L. Valdevit, Energy dissipation mechanisms in hollow metallic microlattices, Journal of Materials Research 29 (16) (2014) 1755–1770.

[55] L. R. Meza, S. Das, J. R. Greer, Strong, lightweight, and recoverable three-dimensional ceramic nanolattices, Science 345 (6202) (2014) 1322–1326.

[56] J. Ma, Z. You, Energy absorption of thin-walled square tubes with a pre-folded origami pattern—part i: geometry and numerical simulation, Journal of Applied Mechanics 81 (1) (2014) 011003.

[57] S. Li, H. Fang, S. Sadeghi, P. Bhovad, K.-W. Wang, Architected origami materials: How folding creates sophisticated mechanical properties, Advanced Materials 31 (5) (2019) 1805282.

[58] T. A. Schaedler, A. J. Jacobsen, A. Torrents, A. E. Sorensen, J. Lian, J. R. Greer, L. Valdevit, W. B. Carter, Ultralight metallic microlattices, Science 334 (6058) (2011) 962–965.

[59] J. L. Silverberg, A. A. Evans, L. McLeod, R. C. Hayward, T. Hull, C. D. Santangelo, I. Cohen, Using origami design principles to fold reprogrammable mechanical metamaterials, science 345 (6197) (2014) 647–650.

[60] S. Shan, S. H. Kang, J. R. Raney, P. Wang, L. Fang, F. Candido, J. A. Lewis, K. Bertoldi, Multistable architected materials for trapping elastic strain energy, Advanced Materials 27 (29) (2015) 4296–4301.

[61] K. Bertoldi, Harnessing instabilities to design tunable architected cellular materials, Annual Review of Materials Research 47 (2017) 51–61.

[62] T.-C. Lim, Negative thermal expansion in transversely isotropic space frame trusses, physica status solidi (b) 250 (10) (2013) 2062–2069.

[63] D. G. Gilmore, Spacecraft thermal control handbook (2002), vol. 1—fundamental technologies .(pp. 373-403), American Institute of Aeronautics and Astronautics. Online version available at: http://www. knovel. com/knovel2/Toc. jsp.

[64] Q. Zhang, J. Wommer, C. O'Rourke, J. Teitelman, Y. Tang, J. Robison, G. Lin, J. Yin, Origami and kirigami inspired self-folding for programming three-dimensional shape shifting of polymer sheets with light, Extreme Mechanics Letters 11 (2017) 111–120.

[65] Y. Mao, Z. Ding, C. Yuan, S. Ai, M. Isakov, J. Wu, T. Wang, M. L. Dunn, H. J. Qi, 3d printed reversible shape changing components with stimuli responsive materials, Scientific reports 6 (2016) 24761.

[66] J. B. Hopkins, K. J. Lange, C. M. Spadaccini, Designing microstructural architectures with thermally actuated properties using freedom, actuation, and constraint topologies, Journal of Mechanical Design 135 (6) (2013) 061004.

[67] S. Tibbits, Design to self-assembly, Architectural Design 82 (2) (2012) 68–73.

[68] J. C. Breger, C. Yoon, R. Xiao, H. R. Kwag, M. O. Wang, J. P. Fisher, T. D. Nguyen, D. H. Gracias, Self-folding thermo-magnetically responsive soft microgrippers, ACS applied materials & interfaces 7 (5) (2015) 3398–3405.

[69] G. Stoychev, N. Puretskiy, L. Ionov, Self-folding all-polymer thermoresponsive microcapsules, Soft Matter 7 (7) (2011) 3277–3279.

[70] R. Lakes, Dense solid microstructures with unbounded thermal expansion, Journal of the Mechanical Behavior of Materials 7 (2) (1996) 85–92.

[71] J. Lehman, R. S. Lakes, Stiff, strong, zero thermal expansion lattices via material hierarchy, Composite Structures 107 (2014) 654–663.

[72] Q. Wang, J. A. Jackson, Q. Ge, J. B. Hopkins, C. M. Spadaccini, N. X. Fang, Lightweight mechanical metamaterials with tunable negative thermal expansion, Physical review letters 117 (17) (2016) 175901.

[73] C. A. Steeves, S. L. d. S. e Lucato, M. He, E. Antinucci, J. W. Hutchinson, A. G. Evans, Concepts for structurally robust materials that combine low thermal expansion with high stiffness, Journal of the Mechanics and Physics of Solids 55 (9) (2007) 1803–1822.

[74] G. Jefferson, T. A. Parthasarathy, R. J. Kerans, Tailorable thermal expansion hybrid structures, International Journal of Solids and Structures 46 (11-12) (2009) 2372–2387.

[75] O. Sigmund, S. Torquato, Composites with extremal thermal expansion coefficients, Applied Physics Letters 69 (21) (1996) 3203–3205.

[76] O. Sigmund, S. Torquato, Design of materials with extreme thermal expansion using a three-phase topology optimization method, Journal of the Mechanics and Physics of Solids 45 (6) (1997) 1037–1067.

[77] S. Watts, D. A. Tortorelli, Optimality of thermal expansion bounds in three dimensions, Extreme Mechanics Letters 12 (2017) 97–100.

[78] J. Qu, M. Kadic, M. Wegener, Poroelastic metamaterials with negative effective static compressibility, Applied Physics Letters 110 (17) (2017) 171901.

[79] J. Qu, M. Kadic, A. Naber, M. Wegener, Micro-structured two-component 3d metamaterials with negative thermal-expansion coefficient from positive constituents, Scientific reports 7 (2017) 40643.